Destruction of spiral waves in chaotic media

Meng Zhan[1,*] and Raymond Kapral[1,†]
[1]*Chemical Physics Theory Group, Department of Chemistry, University of Toronto, Toronto, Ontario M5S 3H6, Canada*
(Received 8 November 2005; published 24 February 2006)

Spiral-wave breakup in strongly chaotic media with nonphase-coherent chaotic attractors is investigated. Spiral-wave dynamics is studied for the Rössler reaction diffusion equation as the local attractor changes from a phase-coherent to a funnel form. Stable spiral waves with an Archimedean structure are observed to persist even when the local chaotic attractor has a funnel form. The destruction of funnel spiral waves in strongly chaotic media is induced by the strong phase disturbance of the local nonlinear chaotic dynamics, which breaks the stable Archimedean spiral structure and globally destroys the spatial pattern.

DOI: 10.1103/PhysRevE.73.026224 PACS number(s): 05.45.Xt, 47.54.−r, 82.40.Ck

I. INTRODUCTION

Spiral waves are often observed in excitable and oscillatory media and the mechanisms responsible for their appearance are well understood [1–3]. They have been studied extensively in laboratory experiments on chemically reacting systems [4,5], fluid convection [6], and in many biochemical and physiological contexts [7,8]. In some situations, it is the mechanisms that lead to the destruction of spiral waves that are important [9]. For example, the breakup of electrochemical spiral-wave patterns in excitable cardiac tissue are believed to be responsible for some types of arrhythmias in the heart, and the instabilities of spiral waves in the Belousov-Zhabotinsky (BZ) reaction lead to chemical turbulence.

Not only can spiral waves arise in excitable and oscillatory media but, somewhat surprisingly, they persist even in media where the underlying dynamics has a complex oscillatory character or is chaotic [10]. An example of a spiral wave in a chaotic system is shown in Fig. 1(a) for the Rössler reaction-diffusion system [11],

$$\partial_t \mathbf{c}(\mathbf{r},t) = \mathbf{R}[\mathbf{c}(\mathbf{r},t)] + D\nabla^2 \mathbf{c}(\mathbf{r},t), \tag{1}$$

where $\mathbf{c}(\mathbf{r},t)$ denotes the set of local concentrations, D is the diffusion coefficient, $\mathbf{R}[c(\mathbf{r},t)]$ represents the local reaction rate and is given by [12] $R_x=-c_y-c_z$, $R_y=c_x+ac_y$, $R_z=(c_x-b)c_z+c$. We see that a well-defined spiral wave exists although the dynamics at a representative spatial point, shown as a (c_x,c_y)-phase-plane plot in Fig. 1(c), has the structure of a chaotic attractor. Spiral waves where the underlying dynamics is complex have not only been seen in simulations on model reaction-diffusion systems, but have also been observed experimentally in the BZ reaction under conditions where the medium undergoes period-doubling bifurcations to chaos [13,14].

Chaotic spiral waves are unusual in that the amplitude field evolves chaotically in space and time but the system maintains phase coherence. Thus, the existence of chaotic spiral waves is connected with the phenomenon of phase synchronization in chaotic media [15]. Although the system may be chaotic it is often possible to define a phase and the resulting phase coherence is responsible for the existence of the spiral wave. Investigations of spiral waves in chaotic media have focused on systems where the local chaotic attractor has a phase-coherent structure, such as that shown in Fig. 1(c). This projection of the local attractor on the (c_x,c_y) plane shows why the phase is easily defined while the amplitude varies chaotically. For an attractor with this structure the phase may be defined by $\theta=\arctan(c_y/c_x)$.

As the parameter a in the Rössler reaction-diffusion system increases, the spiral wave develops a more irregular

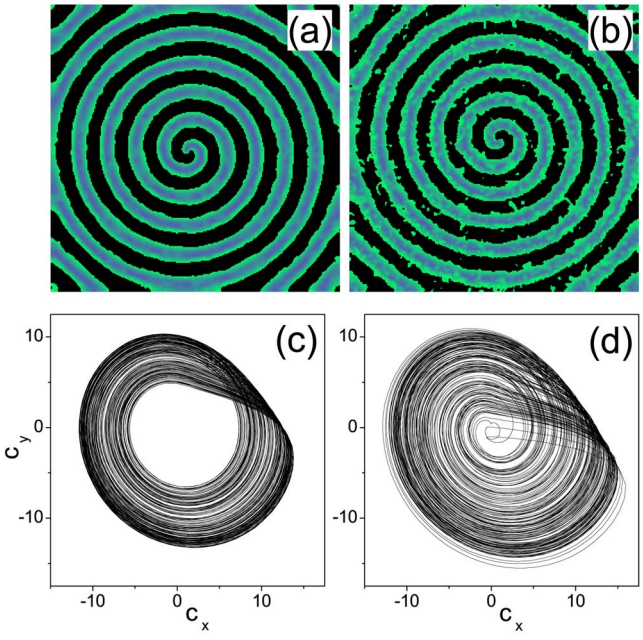

FIG. 1. (Color online) Plot of the $c_x(\mathbf{r},t)$ field at one time instant for (a) $a=0.15$ showing a well defined spiral wave. The dynamics in the (c_x,c_y) plane at a representative spatial point in the medium, far from the spiral core and system boundaries, is shown in panel (c). Panel (b) shows a perturbed spiral wave for $a=0.225$. The corresponding local dynamics is shown in panel (d). The b and c parameters in the Rössler model were fixed at $b=8.5$ and $c=0.4$ and the diffusion coefficient was taken to be $D=0.1$. The b, c, and D values will not be changed for the remainder of the results presented in this paper.

*Electronic address: mzhan@chem.utoronto.ca
†Electronic address: rkapral@chem.utoronto.ca

structure with clearly discernible perturbations [Fig. 1(b)], and the local chaotic attractor adopts a "funnel" form [16] [Fig. 1(d)], where the trajectory makes several loops in phase space in the course of reinjection to the vicinity of the unstable fixed point. One can see that there is still a large degree of phase coherence in the structure of the local attractor for this a value. As a is increased to values higher than $a=0.225$ in Fig. 1(b), the spiral wave becomes even more irregular and the funnel character of the local attractor becomes even more pronounced. For fully developed funnel attractors, and other chaotic attractors whose phase space structure is not simple, the formulation of a generally applicable definition of the phase is a challenging problem [17–19]. For more complex attractors, a phase definition based on considerations of the tangent space structure of the chaotic attractor has been developed [18]. Using such a phase definition, $\theta=\arctan(\dot{c}_y/\dot{c}_x)$, for the Rössler funnel attractor, the nature of the transition to chaotic phase synchronization was studied [18]. A recurrence method, which is believed to be capable of detecting the existence of a phase variable for non-phase-coherent and nonstationary data, has also been proposed [19].

Chaotic attractors lacking phase coherence are commonly observed, for instance, in experiments on chemical reacting systems [20] and nonlinear optical systems [21]. Consequently, it is of interest to investigate the nature of spiral-wave dynamics in systems where the local attractors develop a non-phase-coherent form. As phase coherence in the local attractor is lost, one might expect that such a structural change in the local attractor will lead to the destruction of the chaotic spiral. Based on the appearance of a second extremum in the return map constructed from the local dynamics, our simulations have shown that the local Rössler attractor develops a funnel form at $a=a_{c0}\approx 0.2045$ [22]. Thus, as Fig. 1(b) shows, simple lack of phase coherence as a result of the development of a local funnel attractor is not sufficient to destroy the spiral wave. Spiral breakup occurs only when the local dynamics develops more complex chaotic structure and we now describe the mechanisms leading to spiral destruction in strongly chaotic media.

II. FUNNEL SPIRAL DESTRUCTION

To investigate the breakup of a funnel spiral wave, we start from a single spiral wave that occupies the entire spatial domain and is stable for small values of the Rössler a parameter. The parameter a is then adiabatically increased, using the final configuration as the initial state for the subsequent simulation. From such simulations we find that there is a critical value of a, $a_{c1}\approx 0.228$, beyond which the single funnel spiral wave is no longer stable. For values of $a>a_{c1}$ the system exhibits spatio-temporal turbulence whose character is discussed in the next section.

In oscillatory and excitable media two types of spiral breakup [3,4,9] have been observed, both in simulations and in experiments: a spiral-wave breakup that originates in the core region via a Doppler instability arising from spiral wave meander, and a far-field spiral-wave breakup that first occurs far from the core through a long-wavelength modulation due to an Eckhaus instability [9]. In both cases, before the instability, the spiral waves possess a well-developed modulated spiral structure (superspiral). In contrast, the funnel spiral wave retains its original global spiral form, except the spiral structure is perturbed by apparently homogeneously distributed local disturbances [see Fig. 1(b) for $a=0.225\lesssim a_{c1}\approx 0.228$, and compare it with Fig. 1(a)]. The nature of the spiral instability can also be deduced from observations of the transient evolution leading to spiral breakup following a parameter change; for example, the evolution following a shift of the parameter a from $a=0.2275$, where a stable spiral exists, to $a=0.229>a_{c1}$, shows that the newly formed defects appear in all regions of space, rather than in specific spatial regions such as the core or far-field regions as in the other spiral breakup scenarios.

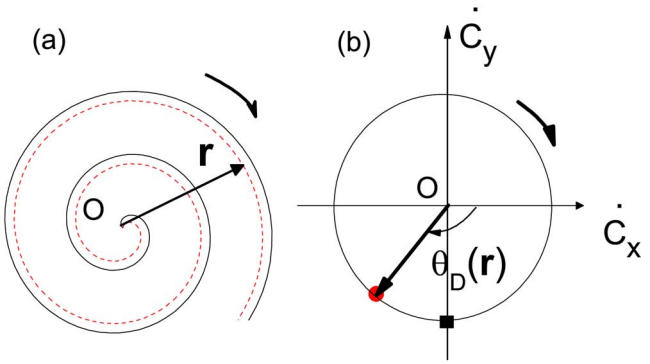

FIG. 2. (Color online) Schematic diagram illustrating the definitions of the spiral phase and dynamic phase (see text for details). In panel (a), the solid curve denotes the reference Archimedean spiral parametrized by the spiral pitch P and initial phase $\theta_{A,0}$. Any spatial point $\mathbf{r}$ in the medium lies on an Archimedean spiral (dashed line) but is characterized by another initial phase $\theta_A(\mathbf{r})$. The phase difference $\theta_A(\mathbf{r})-\theta_{A,0}$ is termed the spiral phase. In panel (b), one turn of the chaotic trajectory at a spatial point $\mathbf{r}$ is schematically represented by a circle in the $(\dot{c}_x,\dot{c}_y)$ plane. The dynamic phase at this point is $\theta_D(\mathbf{r})$. The dynamic phase $\theta_{D,0}=\pi/2$ corresponding to the reference Archimedean spiral is shown as a square.

The mechanism responsible for spiral-wave breakup can be understood by examining the nature of the local phase field in more detail. It is well known that, except very close to the core, spiral waves in simple oscillatory or excitable media take the form of an Archimedean spiral,

$$\rho=\frac{P}{2\pi}(\theta-\theta_{A,0}), \tag{2}$$

shown schematically as the solid curve in Fig. 2(a). Here P is the pitch, ρ and θ are polar coordinates $(+\infty>\theta>\theta_{A,0})$, and $\theta_{A,0}$ is the initial angle with respect to a reference axis with clockwise (the spiral rotation direction) chosen as the positive direction. Spiral waves in chaotic media, such as those shown in Figs. 1(a) and 1(b), are also Archimedean spirals. Each spatial point $\mathbf{r}$ in the medium will lie on an Archimedean spiral of the form of Eq. (2) [the dashed curve in Fig. 2(a)],

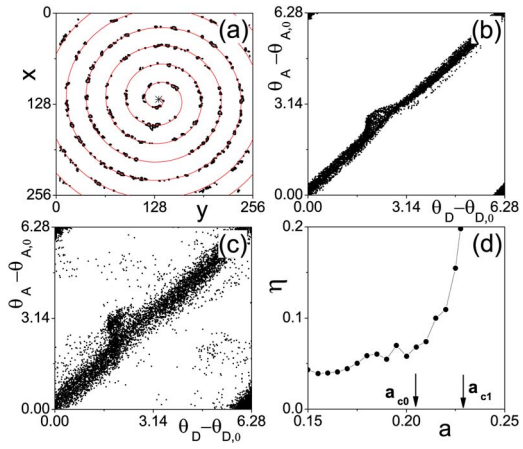

FIG. 3. (Color online) (a) Black points are a plot of the spiral contour line in the coordinate plane for $c_x=-10.0$, a local minimum of c_x. The solid line is a fit of an Archimedean spiral to these points. The spiral tip is denoted by a big star. The Rössler parameter is $a=0.225$. Panels (b) and (c) plot the phase difference $\theta_A-\theta_{A,0}$ versus $\theta_D-\theta_{D,0}$ for $a=0.15$ and 0.225, respectively. Panel (d) plots η versus a with critical parameter a_{c0} and a_{c1}, determined from the correlation function analysis, indicated by arrows.

$$\rho(\mathbf{r}) = \frac{P}{2\pi}[\theta(\mathbf{r}) - \theta_A(\mathbf{r})], \tag{3}$$

but with an initial phase $\theta_A(\mathbf{r})$ that differs from $\theta_{A,0}$. Thus, the difference of angles, $\theta_A(\mathbf{r})-\theta_{A,0}$, which we call the *spiral phase* at point $\mathbf{r}$, connects any spatial point with the reference Archimedean spiral in Eq. (2). For the Rössler system, without loss of generality, we may select the minimum of c_x, e.g., $c_x=-10.0$, to define this reference Archimedean spiral. The reference spiral corresponding to Fig. 1(b) for $a=0.225$ was constructed by using the numerical method of Belmonte *et al.* [4] and is shown in Fig. 3(a). Apart from some dispersion arising from perturbations inherent in the funnel spiral wave, the Archimedean structure of the spiral wave is evident. The two parameters, P and $\theta_{A,0}$, were determined from the fit and $\theta_A(\mathbf{r})$ was obtained from $([\rho(\mathbf{r}),\theta(\mathbf{r})])$ at point $\mathbf{r}$ using Eq. (3).

Since the phase space trajectory of the system is chaotic at any spatial point $\mathbf{r}$, it is often difficult to give a general definition of the phase [17]. We noted earlier that for the Rössler attractor the definition $\theta_D(\mathbf{r})=\arctan(\dot{c}_y/\dot{c}_x)$ [18] has wider applicability than a definition involving phase space variables. Consequently we let $\theta_D(\mathbf{r})$ defined by this equation be the dynamic phase. This definition relies on the assumption that the projection on the $(\dot{c}_x,\dot{c}_y)$ plane is a curve cycling monotonically around a certain point, and, therefore, the phase is a monotonically growing function of time [18]. Clockwise is chosen as the positive direction. For points defining the reference Archimedean spiral, the dynamic phase in the (c_x,c_y) phase plane is approximately equal to π since $c_x=-10$ and $c_y\approx 0$. Therefore, we have $\theta_{D,0}\approx\pi/2$ in the tangent space $(\dot{c}_x,\dot{c}_y)$ [see the square in the tangent space of $(\dot{c}_x,\dot{c}_y)$ in Fig. 2(b)].

If the local dynamics is periodic, the spiral phase defined in coordinate space determines the lag time between the dynamics at the spatial point $\mathbf{r}$ and the reference Archimedean spiral [see the difference between the solid and dashed curves in Fig. 2(a)]. This idea was used to construct an Archimedean spiral splay field theory for spiral dynamics in complex-oscillatory media [23]. For harmonic oscillations, the lag time is controlled by the dynamic phase difference [shown as the phase difference between the circle and square in Fig. 2(b)], and this is also approximately true for the phase-coherent, or even non-phase-coherent, Rössler attractor. This statement is confirmed by the results in Fig. 3(b) which plots $\theta_A(\mathbf{r})-\theta_{A,0}$ versus $\theta_D(\mathbf{r})-\theta_{D,0}$ for $a=0.15$ for all spatial points, excluding the core and boundary points. These points (plotted modulo 2π) lie close to the diagonal indicating strong correlation between the spiral and dynamic phases. (The small "bump" on the diagonal near π is due to the influence of nonzero c_z values.) Note that the choice of the reference Archimedean spiral in Eq. (2) is arbitrary. With increasing a, the approximate equality of $\theta_A-\theta_{A,0}$ and $\theta_D-\theta_{D,0}$ gradually becomes poorer [see Fig. 3(c) for $a=0.225$].

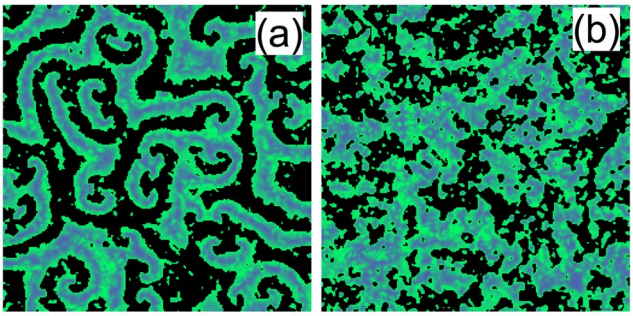

FIG. 4. (Color online) (a) Weak spiral turbulent state for $a=0.235$ and (b) strong turbulence for $a=0.26$.

The function $\eta=<\|\Delta\theta(\mathbf{r})\|^2>$, where $\Delta\theta(\mathbf{r})=[\theta_A(\mathbf{r})-\theta_{A,0}]-[\theta_D(\mathbf{r})-\theta_{D,0}]$, may be used to characterize the deviation from the diagonal. Here $\|\Delta\theta\|=|\Delta\theta|$, for $-\pi\leqslant\Delta\theta\leqslant\pi$ and $2\pi-|\Delta\theta|$ otherwise, and $<>$ indicates a spatial average. The plot of this function in Fig. 3(d) shows that the phase disturbance increases as a is tuned to lie deeper in the chaotic funnel region until the critical parameter $a_{c1}=0.228$ is reached from below. We also observe that there is a discernible change from a slow increase to a very rapid increase in the region of $a_{c0}<a<a_{c1}$. Recall that a_{c0} signals the change from phase-coherent to funnel chaotic attractors.

The above results show that the funnel spiral breakup mechanism differs from the core and far-field mechanisms for spiral breakup described earlier. No spatial modulation of the spiral signals its breakup. The equality (or approximate equality) of the dynamic phase (the strength of the local phase irregularity) and the spiral phase (the strength of the global spiral structure) appears to be a necessary condition for a stable spiral wave, even for the funnel chaotic spiral. When the degree of the local phase irregularity becomes strong enough, deep into the funnel parameter region, breakup of spiral wave occurs.

III. TURBULENT REGIMES

We next briefly consider the turbulent regimes that arise as a result of the breakup of the funnel spiral wave. For

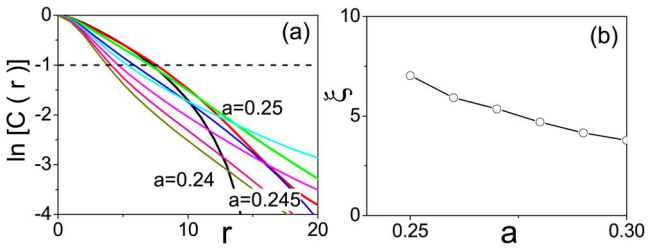

FIG. 5. (Color online) (a) Plot of the spatial correlation function $\ln(C(r))$ versus r showing the crossover from weak to strong turbulence. (b) The spatial correlation length ξ versus a for $a > a_{c2}$.

$a > a_{c1} = 0.228$ the single chaotic spiral wave breaks up into a weakly turbulent state consisting of a large number of small distorted spirals as shown in Fig. 4(a). If a is increased further, beyond $a_{c2} \approx 0.25$ one observes strong turbulence where all vestiges of the spiral structure is lost. Such a turbulent state is shown in Fig. 4(b). Turbulent states with these characteristic features have been observed in the complex Ginzburg-Landau equation [24] and in experiments on the BZ reaction [4]. Both the transition to weak turbulence at a_{c1} and the transition to strong turbulence at a_{c2} occur after the development of the local funnel attractor at a_{c0}.

The transition from weak to strong turbulence at a_{c2} is signaled by a qualitative change in the structure of the spatial correlation function,

$$C(r) = \frac{\langle \delta c_x(\mathbf{r}',t)\, \delta c_x(\mathbf{r}'+\mathbf{r},t)\rangle_{t,\mathbf{r}'}}{\langle \delta c_x(\mathbf{r}',t)^2\rangle_{t,\mathbf{r}'}}, \tag{4}$$

where $\delta c_x(\mathbf{r},t) = c_x(\mathbf{r},t) - \langle c_x(\mathbf{r},t)\rangle_{\mathbf{r},t}$ and the angular brackets denote an average over time and space. In Fig. 5(a) the logarithmic plots of the correlation function are presented and, from right to left above the dashed line, they correspond to $a = 0.24$, 0.245, 0.25, 0.26, …, 0.30, respectively. The crossover through the second critical parameter at $a = a_{c2} = 0.25$ is apparent in this figure from the change in slope of the lines. The spatial correlation length ξ was determined from the intersection of the curves with $\ln[C(r)] = -1$, as $C(r) \propto \exp(-r/\xi)$ for $a > a_{c2}$. The dependence of ξ on a with open circles is plotted in Fig. 5(b); The correlation length decreases gradually for $a > a_{c2}$, as can be seen in the figure, reflecting the increase in spatial disorder as the system parameters are changed to lie deeper in the chaotic regime. We note that the same critical parameter values, $a_{c1} = 0.228$ and $a_{c2} = 0.25$, are found from an analysis of temporal correlation functions.

IV. CONCLUSION

We have shown that spiral waves persist in a chaotic medium where the local attractor has a funnel structure and is not phase coherent, provided breakdown of phase coherence of the local attractor is not too strong. Sufficiently deep into the funnel attractor region a new type of spiral breakup occurs that has its origin in the chaotic dynamics which breaks the stable Archimedean spiral structure. A weak turbulent state results from the breakup of the funnel spiral wave. Deeper in the chaotic regime, weak turbulence changes to strong turbulence signaled by exponential decay of spatial correlations.

While some aspects of the results presented in this paper are model specific, for example, the numerical values of the critical parameters a_{c0}, a_{c1}, and a_{c2}, other features, such as the transitions to weak and strong turbulence as phase coherence is destroyed, should have general applicability. Thus, we expect that the major qualitative aspects of our study should apply to other physical and model systems possessing non-phase-coherent attractors. Studies of other model systems, such as the Willamowski-Rössler model [25], which has a mass-action chemical basis, and the autocatalator model [26] exhibit spiral-wave states in chaotic and complex-periodic parameter regimes. A modified version of the Rössler system has been used to investigate instabilities in lasers giving rise to non-phase-coherent attractors [21]. Since chaotic physical systems often exhibit non-phase-coherent chaotic attractors in some parameter regimes, our study suggests that it may be possible to find stable spiral-wave states, or chaotic states that originate from spiral-wave breakup, in such systems.

This work was supported in part by grants from the Natural Sciences and Engineering Council of Canada, and the Canadian Network of Centers of Excellence on Mathematics of Information Technology and Complex systems (MITACS).

[1] M. Cross and P. Hohenberg, Rev. Mod. Phys. **65**, 851 (1993).
[2] R. Kapral and K. Showalter, *Chemical Waves and Patterns* (Kluwer, Dordrecht, 1995).
[3] I. S. Aranson and L. Kramer, Rev. Mod. Phys. **74**, 99 (2002).
[4] A. L. Belmonte, Q. Ouyang, and J. M. Flesselles, J. Phys. II **7**, 1425 (1997).
[5] G. Ertl, Adv. Catal. **37**, 213 (1990).
[6] S. W. Morris, E. Bodenschatz, D. S. Cannell and G. Ahlers, Phys. Rev. Lett. **71**, 2026 (1993); K. E. Daniels and E. Bodenschatz, *ibid.* **88**, 034501 (2002).
[7] A. Goldbeter, *Biochemical Oscillations and Cellular Rhythms* (Cambridge University Press, Cambridge, 1996).
[8] A. T. Winfree, *When Time Breaks Down* (Princeton University Press, Princeton, 1987).
[9] Q. Ouyang and J. M. Flesselles, Nature (London) **379**, 143 (1996); Q. Ouyang, H. L. Swinney, and G. Li, Phys. Rev. Lett. **84**, 1047 (2000); M. Bar *et al.*, Chaos **4**, 499 (1994); M. Bar and L. Brusch, New J. Phys. **6**, 5 (2004).
[10] A. Goryachev and R. Kapral, Phys. Rev. Lett. **76**, 1619 (1996); A. Goryachev, H. Chate, and R. Kapral, Int. J. Bifurcation Chaos Appl. Sci. Eng. **9**, 2243 (1999); J. Davidsen and R. Kapral, Phys. Rev. Lett. **91**, 058303 (2003); J. Davidsen, R.

Erichsen, R. Kapral, and H. Chate, *ibid.* **93**, 018305 (2004).
[11] The simulations were performed using the explicit Euler method on a 256×256 square domain with no-flux boundary conditions. The space and time steps were $\Delta x = 1.0$ and $\Delta t = 0.02$.
[12] O. Rossler, Ann. N.Y. Acad. Sci. **316**, 376 (1979).
[13] J. S. Park and K. J. Lee, Phys. Rev. Lett. **83**, 5393 (1999); **88**, 224501 (2002); J. S. Park, S. J. Woo, and K. J. Lee, *ibid.* **93**, 098302 (2004).
[14] H. Guo, L. Li, H. Wang, and Q. Ouyang, Phys. Rev. E **69**, 056203 (2004).
[15] A. S. Pikovsky, M. G. Rosenblum, and J. Kurths, *Synchronization-A Unified Approach to Nonlinear Science* (Cambridge University Press, Cambridge, 2001).
[16] E. F. Stone, Phys. Lett. A **163**, 367 (1992).
[17] T. Yalcinkaya and Y. C. Lai, Phys. Rev. Lett. **79**, 3885 (1997); G. Hu, J. Z. Yang, W. Q. Ma, and J. H. Xiao, *ibid.* **81**, 5314 (1998); D. J. DeShazer, R. Breban, E. Ott, and R. Roy, *ibid.* **87**, 044101 (2001).
[18] G. V. Osipov, B. Hu, C. Zhou, M. V. Ivanchenko, and J. Kurths, Phys. Rev. Lett. **91**, 024101 (2003); J. Y. Chen, K. W. Wong, and J. W. Shuai, Phys. Lett. A **285**, 312 (2001).
[19] M. C. Romano, M. Thiel, J. Kurths, I. Z. Kiss, and J. L. Hudson, Europhys. Lett. **71**, 466 (2005).
[20] J. L. Hudson, M. Hart, and D. Marinko, J. Chem. Phys. **71**, 1601 (1979); J. L. Hudson and J. C. Mankin, *ibid.* **74**, 6171 (1981); J. C. Roux, A. Rossi, S. Bachelart, and C. Vidal, Phys. Lett. **A77**, 391 (1980).
[21] J. R. Terry, Int. J. Bifurcation Chaos Appl. Sci. Eng., **12**, 495 (2002).
[22] The critical value of a_{c0} at which the transition to a local funnel-shaped attractor occurs is approximately the same as that for the ordinary differential equation.
[23] M. Zhan and R. Kapral, Phys. Rev. E **72**, 046221 (2005).
[24] H. Chate and P. Manneville, Physica A **224**, 348 (1996).
[25] K. D. Willamowski and O. E. Rössler, Z. Naturforsch. A **35**, 317 (1980).
[26] B. Peng, S. K. Scott, and K. Showalter, J. Phys. Chem. **94**, 5243 (1990); R. Kapral and X. G. Wu, Physica D **103**, 314 (1997).